Evidence of Large Magnetostructural Effects in Austenitic Stainless Steels

L. Vitos,[1,2] P. A. Korzhavyi,[1] and B. Johansson[1,2,3]

[1]*Applied Materials Physics, Department of Materials Science and Engineering, Royal Institute of Technology, SE-10044 Stockholm, Sweden*

[2]*Condensed Matter Theory Group, Physics Department, Uppsala University, S-75121 Uppsala, Box 530, Sweden*

[3]*AB Sandvik Materials Technology, SE-811 81 Sandviken, Sweden*

(Received 20 September 2005; published 24 March 2006)

The surprisingly low magnetic transition temperatures in austenitic stainless steels indicate that in these Fe-based alloys magnetic disorder might be present at room temperature. Using a first-principles approach, we have obtained a theoretical description of the stacking fault energy in $Fe_{100-c-n}Cr_cNi_n$ alloys as a function of composition and temperature. Comparison of our results with experimental databases provides a strong evidence for large magnetic fluctuations in these materials. We demonstrate that the effects of alloying additions on the structural properties of steels contain a dominant magnetic contribution, which stabilizes the most common austenitic steels at normal service conditions.

DOI: 10.1103/PhysRevLett.96.117210 PACS numbers: 75.50.Bb, 71.15.Nc, 81.05.Zx

Fully austenitic stainless steels are composed mainly of Fe, Cr, and Ni, and have the face centered cubic (fcc) crystallographic structure of γ-Fe. At low temperatures, these alloys exhibit a rich variety of magnetic structures as a function of chemical composition, ranging from ferromagnetic phase to spin-glass and antiferromagnetic alignments [1,2]. At ambient conditions the austenitic steels have very low magnetic permeability and are generally regarded as nonmagnetic. Besides the applications where excellent mechanical properties and high corrosion resistance are required, these steels represent the primary choice also for nonmagnetic engineering materials.

It is well known that the local magnetic moments in Fe, Cr, and Ni survive in their high-temperature paramagnetic states [3–10]. The persisting moments give rise to sizable contributions to the specific heat and entropy. These effects were used for tracing the high-temperature spin fluctuations in magnetic transition metals [4,5,11,12]. The magnetic transition temperatures in Fe-rich Fe-Cr-Ni solid solutions are unexpectedly low ($\lesssim 100$ K) [1]. This suggests that in these alloys disordered local magnetic moments might be present at ambient conditions. The picture of nonvanishing magnetic moments in paramagnetic austenitic steels is in line with the high-field magnetization measurements on $Fe_{100-c-n}Cr_cNi_n$ ($14 < n < 21$ and $c = 20$) alloys [2]. These experiments reported Curie-Weiss type susceptibility in the pure paramagnetic regime above ~ 130 K. Having in mind the strong crystal field dependence of Fe magnetic moments [6,13,14], we can anticipate a large impact of the magnetic disorder on the cohesive properties of steels. Based on first-principles alloy theories, here we present a direct verification of the spin fluctuations in Fe-Cr-Ni alloys, and reveal the importance of magnetism on the phase stability and mechanical properties of these important materials.

The outstanding mechanical performance of austenitic steels emerges from the intrinsic properties of austenite. The stacking fault energy (SFE) is a key microscopic parameter of this phase. It is used for modeling a vast number of phenomena, e.g., plastic deformation, phase transformations, shape memory effects. Using various techniques, the SFE of austenitic steels has been measured as a function of composition [15–20] and temperature [21–23], and today commonly accepted databases exist. Numerous empirical models focused on the understanding of the principal factors governing the SFE [15,24,25]. According to the pioneering work by Ishida [24], the SFE, to a good approximation, is proportional to the Gibbs energy difference between the hexagonal close-packed (hcp) and fcc phases. The magnetic free energy vanishes in the hcp Fe (ε-Fe) [6] indicating that the local moments disappear in this phase. Therefore, the SFE appears to be a perfect candidate for detecting the footprint of room-temperature spin fluctuations on the cohesive properties of austenitic steels.

We used the exact muffin-tin orbitals (EMTO) method [26] to compute the SFE of $Fe_{100-c-n}Cr_cNi_n$ alloys. This method, in combination with the coherent potential approximation (CPA) [27], is suitable for describing the simultaneous presence of the chemical and magnetic disorder in Fe-based random alloys [28–30]. In the present study the paramagnetic phase of the $Fe_{100-c-n}Cr_cNi_n$ alloy was modeled by the quasiternary $(Fe^{\uparrow}_{1/2}Fe^{\downarrow}_{1/2})_{100-c-n} \times (Cr^{\uparrow}_{1/2}Cr^{\downarrow}_{1/2})_c(Ni^{\uparrow}_{1/2}Ni^{\downarrow}_{1/2})_n$ alloy with randomly distributed magnetic moments oriented up ($\uparrow$) and down ($\downarrow$). This approximation accurately describes the effect of loss of the net magnetic moment above the transition temperature [7–9].

The most common stacking fault in an fcc crystal, the so-called intrinsic staking fault, may be viewed as a missing (111) layer from an otherwise perfect lattice. The excess free energy ΔF per unit interface area defines the fault energy γ. Within the axial interaction model [31,32],

 © 2006 The American Physical Society

taking into account interactions between layers up to the third nearest neighbors, ΔF can be obtained from the free energies of the hcp, double hcp (dhcp) and fcc lattices as $\Delta F = F_{\mathrm{hcp}} + 2F_{\mathrm{dhcp}} - 3F_{\mathrm{fcc}}$. The temperature ($T$) dependent magnetic moment $\mu(T)$, representing the set of local magnetic moments, was determined from the minimum of the free energy $F(T, \mu) = E(T, \mu) - T[S^{\mathrm{mag}}(\mu) + S^{\mathrm{el}}(T)]$ calculated at the theoretical equilibrium volume. The electronic energy $E(T, \mu)$ and entropy $S^{\mathrm{el}}(T)$ were obtained from spin-constrained EMTO-CPA calculations, using the finite-temperature Fermi distribution. The magnetic entropy was calculated using the mean-field expression $S^{\mathrm{mag}} = k_{\mathrm{B}} \log(\mu + 1)$ (k_{B} is the Boltzmann constant) valid for completely disordered localized moments [4]. The phonon contribution to ΔF was neglected, which is estimated to introduce an error $\lesssim 2$ mJ/m^2 in γ [33], and $\lesssim 0.3\%$ per atomic percent Fe in the composition dependence of γ [36]. The one-electron equations were solved within the scalar-relativistic and frozen-core approximations, and the Green function was calculated for 52 complex energy points. In the basis set we included s, p, d, and f orbitals. In the irreducible wedge of the fcc, hcp and dhcp Brillouin zones we used 1000–1500 uniformly distributed k points. The error associated with the above numerical approximations was found to be ~ 0.1 mJ/m^2 in γ. The exchange-correlation term was treated within the generalized gradient approximation [37]. Because of the reduced diffusion rate at low temperatures, the experimental SFE are considered to represent nonequilibrium values corresponding to homogeneous distribution of alloying elements [24]. Accordingly, in our study the Suzuki segregation effects were omitted.

In Fig. 1(a), we compare the theoretical SFE calculated at 300 K with room-temperature experimental data [15–20]. Taking into account the error bars reported in the measurements and the effect of the trace substitutional elements (e.g., Mo, Si, Mn) present in the experimental samples, the agreement between theory and experiment is very good. The deviations are somewhat larger for alloys with theoretical γ below 10 mJ/m^2. These alloys correspond to low-Ni austenite containing small amount of C and N. These elements occupy interstitial positions, and are known to enhance the SFE of austenitic steels [19]. The calculated temperature dependence of the SFE for two compositions, close to those considered in the experiments [21–23], is shown in Fig. 1(b). The large γ versus temperature slope obtained in the experiments (~ 10 mJ/m^2 per 100 K) is very well reproduced by the present theory. For all data, $\partial\gamma/\partial T$ slightly decreases with T, showing a tendency to saturate at high temperatures. The general good agreement between the theoretical and experimental data from Fig. 1 illuminates that our model correctly accounts for the main factors governing the SFE. Therefore, we feel confident using this model to shed light on the role of magnetism on the structural and mechanical properties of austenitic steels.

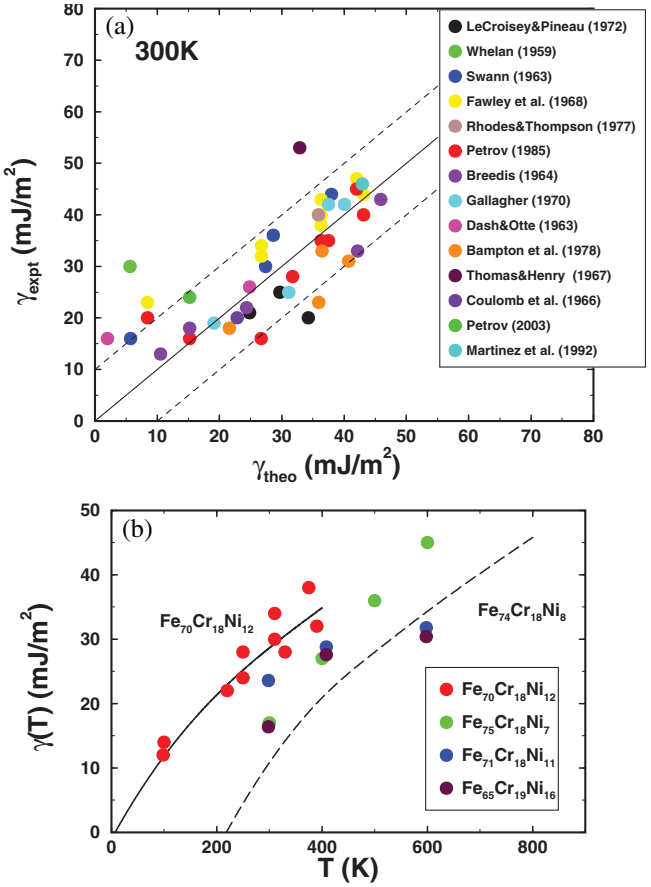

FIG. 1 (color). Comparison between the theoretical and experimental stacking fault energies for austenitic steels. (a) The room-temperature experimental (γ_{expt}) and theoretical (γ_{theo}) SFE for alloys with different chemical compositions. The actual makeup of the alloys can be found in references listed in legend [15–20]. The dashed lines indicate that most of the experimental data are situated within ± 10 mJ/m^2 around γ_{theo}. (b) Temperature dependence of the SFE. Lines stand for the theoretical results for $Fe_{70}Cr_{18}Ni_{12}$ (solid line) and $Fe_{74}Cr_{18}Ni_{8}$ (dashed line). Symbols are the experimental values for $Fe_{70}Cr_{18}Ni_{12}$ [22], $Fe_{71}Cr_{18}Ni_{11}$ and $Fe_{65}Cr_{19}Ni_{16}$ [21], and the average experimental values for $Fe_{75}Cr_{18}Ni_{7}$ [23] with errors of 20 mJ/m^2.

To obtain an insight into the atomic-level mechanism behind the trends of the SFE, in Fig. 2 we present the calculated $\gamma(c, n, T)$ maps for $13.5 < c < 25.5$, $8 < n < 20$, and $T = 0$, 150, and 300 K. The chemical effect on the SFE can be seen on the 0 K map. We find that, at low temperatures, Cr decreases and Ni increases the SFE. These composition-induced variations are in good accordance with the theory of the phase stability of transition metals [38]. According to that theory, decreasing the number of electrons in a stable paramagnetic fcc system leads to a fcc-to-hcp transition. Because Cr addition produces a reduction in the effective number of electrons in the Fe-Cr-Ni alloys, this element stabilizes the hcp structure relative to the fcc structure, and thus decreases the stacking fault

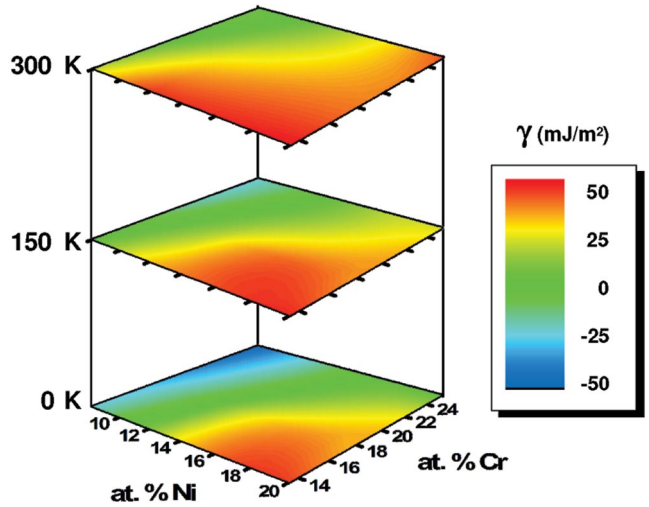

FIG. 2 (color). Stacking fault energy maps of Fe-Cr-Ni random alloys. The calculated SFE is shown as a function of the chemical composition and temperature.

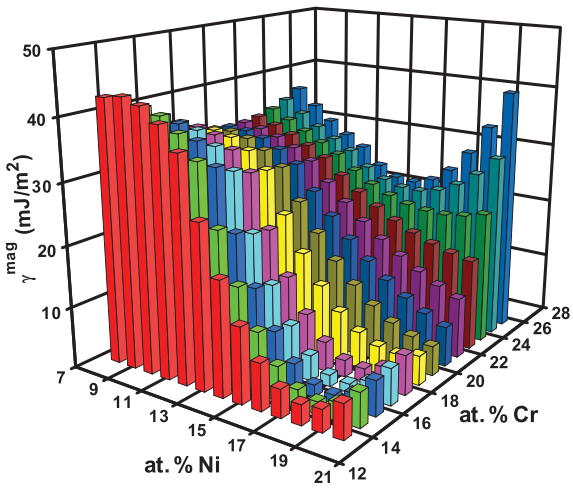

FIG. 3 (color). The magnetic fluctuation contribution to the stacking fault energy. γ^{mag} is plotted for $T = 300$ K as a function of the chemical composition.

energy of the Fe-based alloys. Similarly, a small amount of Ni removal from the Fe-Cr-Ni alloys diminishes the SFE.

Temperature is found to have a remarkable effect on the SFE maps. With increasing temperature, the $\gamma(c, n, T)$ surface becomes smoother than that at 0 K (Fig. 2, 150 and 300 K maps). The ~ 90 mJ/m^2 difference between the largest and the smallest SFE at 0 K decreases to ~ 60 mJ/m^2 at room temperature. This smoothening is mainly due to the pronounced SFE increase at the low-Ni high-Cr corner of the energy map. In the high-Ni low-Cr corner $\gamma(c, n, T)$ shows a weak temperature dependence. The SFE enhancing effect of Ni is retained also at room temperature, with a slightly attenuated $\partial\gamma/\partial n$ slope at high n. On the other hand, the hcp stabilizing effect of Cr at room temperature is limited to low-Ni alloys. For high-Ni alloys ($n \approx 18$–20) the $\partial\gamma/\partial c$ slope is negative for $c < 20$ and positive for $c > 20$. This change is a consequence of the persisting local moments in austenitic steels.

The effect of the Fermi function from the electronic energy and electronic entropy is relatively insignificant at room temperature. Hence, the dominant temperature dependence of γ comes from the $TS^{\mathrm{mag}}(\mu(T))$ term and from the part of the electronic energy that depends on T through $\mu(T)$. This allows us to identify the magnetic fluctuation contribution to the stacking fault energy (γ^{mag}) with the temperature dependent part of γ. Theoretical room-temperature data for γ^{mag} are shown in Fig. 3. We find that the magnetic SFE has the same order of magnitude as the total SFE, confirming the importance of the disordered local moments for the stability of steels. For the entire composition interval considered in the present study, the paramagnetic fcc alloys have large disordered local moments. At 0 K these moments are located on Fe atoms, and have magnitudes per Fe atom ranging from $1.35\mu_{\mathrm{B}}$, near $Fe_{67}Cr_{25}Ni_8$, to $1.75\mu_{\mathrm{B}}$, near $Fe_{67}Cr_{13}Ni_{20}$. The magnetic moments in the dhcp structure are close to those in the fcc structure, and, therefore, the $-2TS^{\mathrm{mag}}_{\mathrm{dhcp}}$ term in γ^{mag} is to a great extent canceled by the $2TS^{\mathrm{mag}}_{\mathrm{fcc}}$ term. The situation is very different for the hcp structure. At the theoretical volumes, the low-Ni hcp alloys are calculated to be nonmagnetic with vanishing local magnetic moments. However, the low γ^{mag} values, found for the low-Cr and high-Ni corner of Fig. 3, indicate that the alloys from this corner of the map have similar S^{mag} in the hcp and fcc phases. Indeed, we find that upon Ni addition the low-Cr hcp alloys undergo a transition from a nonmagnetic to a paramagnetic phase with nonvanishing local moments. At high-Ni and low-Cr contents the hcp alloys possess disordered magnetic moments of $(0.95$–$1.50\mu_{\mathrm{B}})$ per Fe atom. Our calculations show that in contrast to Ni the Cr addition always tends to stabilize the zero local moment solution in the hexagonal phase. For instance, in hcp alloys with $n \approx 18$–20, the local moments disappear with c increasing from 13.5% to 25.5%. This magnetic transition explains the obtained change in the $\partial\gamma/\partial c$ slope from Fig. 2 (300 K map).

Temperature enhances the magnetic moments on Fe sites and induces small disordered moments on Cr and Ni sites. In the fcc alloys, the average room-temperature moments per Fe atom vary from $1.45\mu_{\mathrm{B}}$ to $1.85\mu_{\mathrm{B}}$, corresponding to $Fe_{67}Cr_{25}Ni_8$ and $Fe_{67}Cr_{13}Ni_{20}$, respectively. These figures are somewhat smaller than $(1.97$–$2.31\mu_{\mathrm{B}})$ estimated from the measured Curie-Weiss susceptibility [2]. The effect of temperature is considerable in the hcp alloys close to the magnetic instability. In the case of $Fe_{67}Cr_{17}Ni_{16}$ alloy, for instance, the hcp magnetic moments on the Fe, Cr, and Ni sites increase by approximately $0.95\mu_{\mathrm{B}}$, $0.15\mu_{\mathrm{B}}$, and $0.05\mu_{\mathrm{B}}$, respectively, as the temperature rises from 0 to 300 K. Expressed per Fe atom, these figures correspond to $1.0\mu_{\mathrm{B}}$ change in the average mag-

netic moment, compared to $0.1\mu_B$ change obtained for the fcc phase. The different rate of the thermal fluctuations in fcc and hcp lattices is responsible for the observed nonlinear behavior of $\gamma(T)$ [Fig. 1(b)].

The most widespread austenitic steel grades encompass approximately 18% Cr and 8%–12% Ni, and have Néel temperatures $T_N < 50$ K [1]. We have found that these alloys have very low or negative SFE at temperatures from just above T_N to about 200–250 K. Consequently, at these temperatures the common austenitic steels show instability against fcc-hcp martensitic transformation. Our simulations demonstrate that large magnetic fluctuations are present in these steels. These fluctuations give a substantial magnetic contribution to the fcc-hcp energy balance, stabilizing the austenitic phase near room temperature. Furthermore, we have shown that the observed strong temperature dependence of the SFE for stainless steels [21–23] originates from their magnetism. We conclude that the presence of large disordered magnetic moments in the paramagnetic state can explain a wide diversity of properties that the austenitic stainless steels exhibit. Our findings have important implications for modern materials science, as they clearly show that a consistent approach to materials design must be based on quantum theory and thermodynamics. This combination offers a unique possibility for a thorough control of the balance between competing atomic-level effects.

The Swedish Research Council, the Swedish Foundation for Strategic Research, and The Royal Swedish Academy of Sciences are acknowledged for financial support.

[1] A. K. Majumdar and P. v. Blanckenhagen, Phys. Rev. B **29**, 4079 (1984).
[2] T. K. Nath, N. Sudhakar, E. J. McNiff, and A. K. Majumdar, Phys. Rev. B **55**, 12 389 (1997).
[3] O. Steinsvoll, C. F. Majkrzak, G. Shirane, and J. Wicksted, Phys. Rev. Lett. **51**, 300 (1983).
[4] G. Grimvall, Phys. Rev. B **39**, 12 300 (1989).
[5] G. Grimvall, J. Häglund, and A. Fernandez Guillermet, Phys. Rev. B **47**, R15338 (1993).
[6] G. Grimvall, Phys. Scr. **13**, 59 (1976).
[7] T. Oguchi, K. Terakura, and N. Hamada, J. Phys. F **13**, 145 (1983).
[8] B. L. Györffy, A. J. Pindor, G. M. Stocks, J. Staunton, and H. Winter, J. Phys. F **15**, 1337 (1985).
[9] F. J. Pinski, J. Staunton, B. L. Györffy, D. D. Johnson, and G. M. Stocks, Phys. Rev. Lett. **56**, 2096 (1986).
[10] M. Shimizu, Phys. Lett. **81A**, 87 (1981).
[11] R. J. Weiss and K. J. Tauer, Phys. Rev. **102**, 1490 (1956).
[12] M. Hillert and M. Jarl, CALPHAD: Comput. Coupling Phase Diagrams Thermochem. **2**, 227 (1978).
[13] M. van Schilfgaarde, I. A. Abrikosov, and B. Johansson, Nature (London) **400**, 46 (1999).
[14] T. Asada and K. Terakura, Phys. Rev. B **46**, R13599 (1992).
[15] A. P. Miodownik, CALPHAD: Comput. Coupling Phase Diagrams Thermochem. **2**, 207 (1978).
[16] R. E. Schramm and R. P. Reed, Metall. Trans. A **6**, 1345 (1975).
[17] C. G. Rhodes and A. W. Thompson, Metall. Trans. A **8**, 1901 (1977).
[18] Yu. N. Petrov, Phys. Met. **6**, 735 (1985).
[19] Yu. N. Petrov, Z. Metallkd. **94**, 1012 (2003).
[20] L. G. Martinez, K. Imakuma, and A. F. Padilha, Steel Research **63**, 221 (1992).
[21] R. M. Latanision and A. W. Ruff, Jr., Metall. Trans. **2**, 505 (1971).
[22] G. B. Olson and M. A. Cohen, Metall. Trans. A **7**, 1897 (1976).
[23] F. Abrassart, Metall. Trans. **4**, 2205 (1973).
[24] K. Ishida, Phys. Status Solidi (a) **36**, 717 (1976).
[25] P. J. Ferreira and P. Müllner, Acta Mater. **46**, 4479 (1998).
[26] L. Vitos, I. A. Abrikosov, and B. Johansson, Phys. Rev. Lett. **87**, 156401 (2001).
[27] P. Soven, Phys. Rev. **156**, 809 (1967).
[28] L. Vitos, P. A. Korzhavyi, and B. Johansson, Phys. Rev. Lett. **88**, 155501 (2002).
[29] L. Vitos, P. A. Korzhavyi, and B. Johansson, Nat. Mater. **2**, 25 (2003).
[30] L. Dubrovinsky *et al.*, Nature (London) **422**, 58 (2003).
[31] P. J. H. Denteneer and W. van Haeringen, J. Phys. C **20**, L883 (1987).
[32] C. Cheng, R. J. Needs, and V. Heine, J. Phys. C **21**, 1049 (1988).
[33] We assess the effect of phonon vibrations on the SFE by making the approximation $\Delta F^{ph} \approx F^{ph}_{hcp} - F^{ph}_{fcc}$, i.e., assuming that the fcc and dhcp lattices possess similar vibrational free energies. From the high-temperature expansion of the phonon entropy [4], for two solids with similar Debye temperatures (θ) we have $\Delta F^{ph} \approx 3k_B T(\Delta\theta/\theta)$ [6]. Using the Debye temperature ratios for α-Fe (ferrite) and ε-Fe ($\theta_{bcc}/\theta_{hcp} \approx 0.96$) [34] and for α- and γ-Fe ($\theta_{bcc}/\theta_{fcc} \approx 0.97$) [6,35], at $T = 300$ K we obtain $\Delta F^{ph} \approx 0.75$ meV/atom, which corresponds to ≈ 2 mJ/m^2 vibrational contribution to the SFE.
[34] D. L. Williamson, S. Bukshpan, and R. Ingalls, Phys. Rev. B **6**, 4194 (1972).
[35] G. Grimvall and I. Ebbsjö, Phys. Scr. **12**, 168 (1975).
[36] From the elastic property maps for Fe-Cr-Ni alloys [28], we find that θ_{fcc} [see Ref. [33]] changes by less than 4% when proceeding from $Fe_{78.5}Cr_{13.5}Ni_8$ to $Fe_{54.5}Cr_{25.5}Ni_{20}$. Assuming that θ_{hcp} and θ_{fcc} exhibit similar composition dependences, we find that the average composition-induced variation of ΔF^{ph} is $\lesssim 0.3\%$ per atomic percent Fe.
[37] J. P. Perdew, K. Burke, and M. Ernzerhof, Phys. Rev. Lett. **77**, 3865 (1996).
[38] H. L. Skriver, Phys. Rev. B **31**, 1909 (1985).